TWO-BAND k·p MODEL FOR THE CONDUCTION BAND IN SILICON

Viktor Sverdlov, Gerhard Karlowatz, Hans Kosina, and Siegfried Selberherr
Institute for Microelectronics
Vienna University of Technology
Gußhausstraße 27–29/E360, A-1040 Wien, Austria
e-mail: sverdlov@iue.tuwien.ac.at

KEYWORDS
Silicon band structure, **k·p** theory, mobility, Monte Carlo

ABSTRACT

The modification of the silicon conduction band under uniaxial [110] stress is considered. Special attention is paid to the stress dependence of the non-parabolicity parameter. An analytical expression of the dependence of the non-parabolicity parameter on shear stress is obtained. At 3 GPa stress the non-parabolicity is shown to increase by a factor of 1.7. The stress dependence of the non-parabolicity parameter is verified by comparing the corresponding analytical density-of-states to the numerical density-of-states obtained from the empirical pseudopotential method and good agreement is found. The increase in the non-parabolicity parameter increases the after-scattering density-of-states and the scattering rates, which results in an almost 25% suppression of the mobility enhancement due to the corresponding effective mass decrease in a 3 nm Si body thin FET at 3 GPa [110] stress.

INTRODUCTION

Stress-induced mobility engineering has become a key technique to increase the performance of modern CMOS devices. The reason for the mobility enhancement lies in the band structure modification caused by stress. The conduction band in Si is commonly approximated by three pairs of equivalent valleys with their minima located close to the X-points of the Brillouin zone. Close to the minima the electron dispersion is well described by the effective mass approximation. At higher electron energies the non-parabolicity parameter (typically $\alpha = 0.5$ eV^{-1}) has to be introduced to describe deviations from the density of states of the purely parabolic dispersion.

The semiconductor industry is exploiting stress techniques compatible with existing CMOS process technology. Stress is generated by local stressors and/or additional cap layers. The technologically relevant stress along the [110] direction was systematically investigated experimentally only recently [1]. Inherent to [110] uniaxial stress is a shear distortion of the Si crystal lattice, which induces pronounced modifications in the conduction band. Shear strain produces nonlinear shifts between the valleys [2, 3], and the degeneracy between the six equivalent valleys is lifted. Shear strain also modifies substantially both the longitudinal [2, 3] and transversal [1, 2, 3, 4] effective masses. The transversal mass determines the mobility in a FET with ultra-thin Si body. In such FETs the electron mobility enhancement induced by [110] tensile stress is therefore solely due to a decrease of the conductivity mass in the stress direction [1, 2, 3]. However, a possible stress dependence of the non-parabolicity parameter has not yet been considered.

TWO-BAND k·p THEORY AND NON-PARABOLICITY

We consider the valley along the [001] direction only, other valleys are analyzed in a similar fashion. The closest band to the first conduction band Δ_1 ($i = 1$) is the second conduction band $\Delta_{2'}$ ($i = 2$). The two bands become degenerate exactly at the X points. Since the minimum of the conduction band is only $k_0 = 0.15\frac{2\pi}{a}$ away from the X point, the dispersion around the minimum is well described by degenerate perturbation theory, which includes only these two bands. Diagonal elements of the Hamiltonian H_{ii}at the X point, where $i = 1, 2$ are:

$$H^0_{ii}(k) = (-1)^{i-1}\frac{\hbar}{m_0}k_z p + \frac{\hbar^2 k_z^2}{2m_l} + \frac{\hbar^2 k_x^2}{2m_t} + \frac{\hbar^2 k_y^2}{2m_t}, \quad (1)$$

where m_0 is the free electron mass, m_t is the transversal, and m_l is the longitudinal effective mass. The values of k_z are counted from the X point and are thus negative. The coupling between the two bands is described by the off-diagonal terms [4]:

$$H^0_{12}(k) = \frac{\hbar^2 k_x k_y}{M}. \quad (2)$$

The parameter M can be obtained from **k·p** perturbation theory:

$$\frac{1}{M} = \frac{1}{m_0}\left|\sum_{l\neq 1,2}(p_y)_{1l}(p_z)_{l2}\left(\frac{1}{E_l - E_1} + \frac{1}{E_l - E_2}\right)\right|.$$

We use for M the value computed by the empirical pseudo-potential method (EPM) at the $k_z = -k_0$ point, where the numerical value is close (but not equal) to $M \approx m_t/(1 - m_t/m_0)$ reported in [4]. With degenerate perturbation theory we obtain the following dispersion relation:

$$E(\mathbf{k}) = \frac{\hbar^2 k_z^2}{2m_l} + \frac{\hbar^2(k_x^2 + k_y^2)}{2m_t} - \sqrt{\left(\frac{\hbar}{m_0} k_z p\right)^2 + \left(\frac{\hbar^2 k_x k_y}{M}\right)^2}. \quad (3)$$

Expanding (3) around the minimum $k_z = -k_0$ with respect to $p_z = k_z - k_0$, one obtains a simplified dispersion relation [5]:

$$E(\mathbf{k}) = \frac{\hbar^2 p_z^2}{2m_l} + \frac{\hbar^2(k_x^2 + k_y^2)}{2m_t} - \frac{\left(\hbar^2 k_x k_y\right)^2}{M^2 \Delta} - \frac{\Delta}{4}, \quad (4)$$

where $\Delta = 2\hbar k_0 p/m_0 = 2\hbar^2 k_0^2/m_l$ is the gap between the Δ_1 and the $\Delta_{2'}$ conduction bands at $k_z = -k_0$. To estimate the value of the non-parabolicity parameter, we follow [5], Appendix B, and average out the angular dependence in (4). Assuming $\alpha E(\mathbf{k})$ to be small and recasting terms, one finally obtains:

$$\frac{\hbar^2(k_x^2 + k_y^2)}{2m_t} = E(\mathbf{k})\left(1 + \alpha E(\mathbf{k})\right),$$

with

$$\alpha = \frac{1}{2\Delta}\left(\frac{m_t}{M}\right)^2. \quad (5)$$

Substituting Si parameter values in (5), we estimate $\alpha = 0.6\ \mathrm{eV}^{-1}$, which is close to the phenomenological value of $\alpha = 0.5\ \mathrm{eV}^{-1}$.

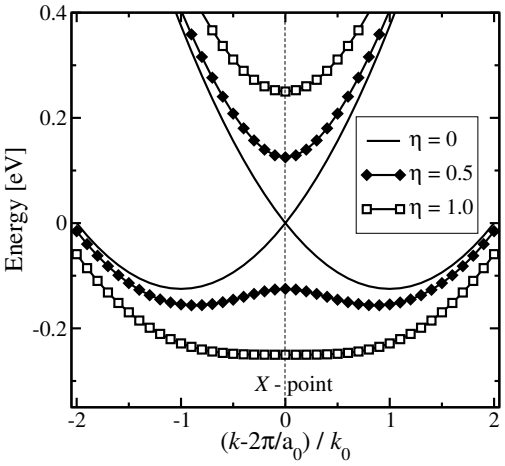

Figure 1: Conduction band profile along [001] for different strain values in [110] direction.

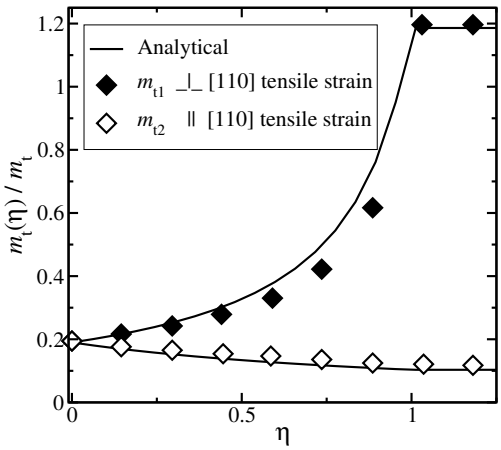

Figure 2: Dependences of the transversal effective mass on shear stress. The mass develops two branches.

CONDUCTION BAND MODIFICATIONS UNDER SHEAR STRAIN

Uniaxial stress along the [110] direction generates diagonal (ε_{ii}) as well as off-diagonal (ε_{xy}) components of the strain tensor in the principal coordinate system. The diagonal components are added to the diagonal matrix elements (1) of the [001] valley [6]:

$$H_{ii} = H_{ii}^0 + \delta E_C, \quad (6)$$

where $\delta E_C = \Xi_d\left(\varepsilon_{xx} + \varepsilon_{yy} + \varepsilon_{zz}\right) + \Xi_u\,\varepsilon_{zz}$, with Ξ_d denoting the dilation and Ξ_u the uniaxial deformation potentials for the conduction band. The off-diagonal elements of the Hamiltonian are modified by the shear strain components [4]:

$$H_{ij}(k) = H_{ij}^0 - D\varepsilon_{xy}, \quad (7)$$

where $D = 14$ eV denotes the shear deformation potential.

The dispersion relation of the [001] valleys including the shear strain component for the conduction band now reads as:

$$E(\mathbf{k}) = \frac{\hbar^2 k_z^2}{2m_l} + \frac{\hbar^2(k_x^2 + k_y^2)}{2m_t} + \delta E_C - \sqrt{\left(\frac{\hbar}{m_0} k_z p\right)^2 + \left(D\varepsilon_{xy} - \frac{\hbar^2 k_x k_y}{M}\right)^2}. \quad (8)$$

Valley shifts

The off-diagonal strain component lifts the degeneracy between the two lowest conduction bands at the X points along the [001] axis. Since the conduction band minimum along the [001] axis is located near the

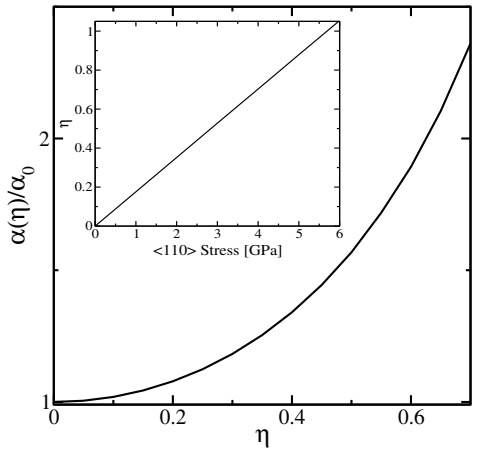

Figure 3: Analytical expression for dependence of the non-parabolicity parameter on stress. Inset: relation between normalized stress and stress in GPa.

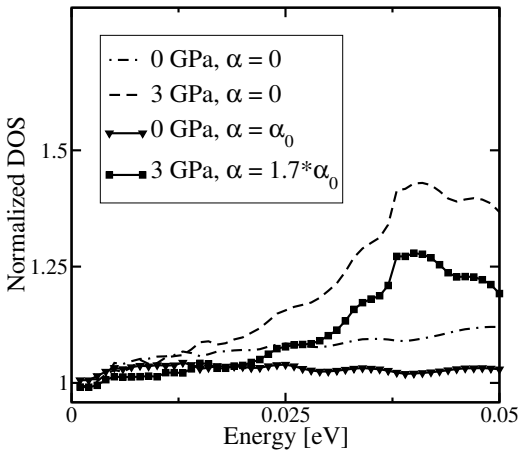

Figure 4: Numerical DOS in [001] valley normalized to the DOS analytical expressions obtained without (dotted lines) and with stress dependent nonarabolicity parameter (solid lines), for unstrained Si and Si under [110] uniaxial stress.

X point, the gap at the X point affects the position of the minimum as illustrated in Fig. 1. The minimum $k_{\min}$ moves closer to the X point. From (8) we obtain

$$k_{\min} = -k_0\sqrt{1-\eta^2}, \quad |\eta| < 1 \tag{9}$$

Here, the dimensionless off-diagonal strain $\eta = 2D\varepsilon_{xy}/\Delta$ is introduced. For $\eta \geq 1$ the valley minimum stays exactly at the X point.
The minimum of the [001] valley moves down in energy with respect to the remaining four fold degenerate valleys. For $\eta \leq 1$ the strain dependence is quadratic, while it is linear for $\eta \geq 1$:

$$\Delta E_{\text{shear}} = \begin{cases} -\dfrac{\Delta}{4}\eta^2 & , \quad |\eta| < 1 \\ -\dfrac{\Delta}{4}(2|\eta| - 1) & , \quad |\eta| > 1 \end{cases} \tag{10}$$

The shifts predicted by (10) were compared with results from EPM calculations and excellent agreement was found.

Stress-dependent effective masses

A shear strain component ε_{xy} modifies the effective masses in the [001] valleys. Evaluating the second derivatives of (8) at the band minimum (13), we obtain two different branches for the effective mass across (m_{t1}) and along (m_{t2}) the stress direction [110]:

$$\frac{m_t}{m_{t1}(\eta)} = \begin{cases} \left(1 - \eta\dfrac{m_t}{M}\right) & , \quad |\eta| < 1 \\ \left(1 - \text{sgn}(\eta)\dfrac{m_t}{M}\right) & , \quad |\eta| > 1 \end{cases} \tag{11}$$

$$\frac{m_t}{m_{t2}(\eta)} = \begin{cases} \left(1 + \eta\dfrac{m_t}{M}\right) & , \quad |\eta| < 1 \\ \left(1 + \text{sgn}(\eta)\dfrac{m_t}{M}\right) & , \quad |\eta| > 1 \end{cases} \tag{12}$$

Here, sgn(η) denotes the sign function. In Fig. 2 the analytical expressions for the transversal masses (11) and (12) are compared with the masses obtained from EPM calculations. To improve the agreement at high values of stress $\eta \approx 1$, the deformation potential D is set to be slightly stress dependent in the form $D(\eta) = D + \beta\eta^2$, with $\beta = 0.7$ eV.

Stress and non-parabolicity

Shear strain affects the value of the non-parabolicity parameter α as well. In order to find the dependence, we rewrite the dispersion relation (8) in the vicinity of the valley minimum $k_{\min}$, which in the case of $k_x, k_y \neq 0$ is equal to

$$k_{\min} = -k_0\sqrt{1 - 4\left(\frac{D\varepsilon_{xy} - \frac{\hbar^2 k_x k_y}{M}}{\Delta}\right)^2}, \tag{13}$$

and, therefore, depends on $k_x k_y$. Expanding (8) around the minimum (13) for small $p_z = k_z - k_{\min}$, one obtains:

$$\begin{aligned} E(\mathbf{k}) = \; & \frac{\hbar^2 p_z^2}{2m_l(\eta)} + \frac{\hbar^2(k_x^2 + k_y^2)}{2m_t} - \frac{\Delta}{4} \\ & - \frac{1}{\Delta}\left(D\varepsilon_{xy} - \frac{\hbar^2 k_x k_y}{M}\right)^2, \end{aligned} \tag{14}$$

Taking into account the shifts of the valley minima (13) and the effective mass changes (11), (12), we rewrite

(14) as

$$E(\mathbf{k}) = \frac{\hbar^2 p_z^2}{2m_l(\eta)} + \frac{\hbar^2 \tilde{k}_x^2}{2m_{t2}(\eta)} + \frac{\hbar^2 \tilde{k}_y^2}{2m_{t1}(\eta)} - \frac{\hbar^4 \left(\tilde{k}_x^2 - \tilde{k}_y^2\right)^2}{2M^2\Delta}, \quad (15)$$

where $\tilde{k}_x = (k_x + k_y)/\sqrt{(2)}$ and $\tilde{k}_y = (k_x - k_y)/\sqrt{(2)}$ are the momentum projections in the rotated coordinate system, where the new x axis is along the [110] stress direction. The non-parabolic term written in the original xy coordinate system is similar to the corresponding term in (4). However, the parabolic term contains the effective masses $m_{t1}(\eta), m_{t2}(\eta)$, which are modified due to [110] stress. Introducing new variables $\tilde{x} = p_x/\sqrt{m_{t2}(\eta)}, \tilde{y} = p_y/\sqrt{m_{t1}(\eta)}$, we separate the renormalization due to stress of the parabolic part of the density-of-states (DOS) from the non-parabolic contribution. One rewrites (4) at $k_z = -k_0(\eta)$ as

$$E(\tilde{x}, \tilde{y}) = \frac{\hbar^2 \left(\tilde{x}^2 + \tilde{y}^2\right)}{2} - \left(m_{t2}(\eta)\tilde{x}^2 - m_{t1}(\eta)\tilde{y}^2\right)^2 \frac{\hbar^4}{2M^2\Delta}. \quad (16)$$

The last term gives the correction to the density of states of the parabolic bands. Assuming the last term to be small, we compute the correction to the DOS identifying it with the isotropic non-parabolicity parameter $\alpha(\eta)$. Taking into account the dependences (11) and (12) of the masses $m_{t1}(\eta), m_{t2}(\eta)$ on the stress η, we arrive at an expression for the strain dependent non-parabolicity parameter $\alpha(\eta)$:

$$\alpha(\eta) = \alpha_0 \frac{1 + 2(\eta m_t/M)^2}{1 - (\eta m_t/M)^2} \quad (17)$$

Expression (17) is plotted in Fig. 3. The non-parabolicity parameter depends on the square of the stress value and therefore does not depend on whether stress is tensile or compressive. This is expected, since tensile stress in [110] direction produces compression along $[1\bar{1}1]$, thus α can not depend on the sign of stress. Due to the quadratic dependence, the relative increase of $\alpha(\eta)$ is more pronounced at relatively large stress values.

RESULTS AND DISCUSSION

Fig. 4 illustrates the density-of-states of the [001] valley as a function of energy relative to the minimum, obtained numerically from empirical pseudo-potential calculations, for the unstressed case and stress equal to 3 GPa. The value of the non-parabolicity parameter at 3GPa is 70% higher than the unstrained value α_0, according to (17). The DOS is normalized to the analytical DOS corresponding to the parabolic dispersion

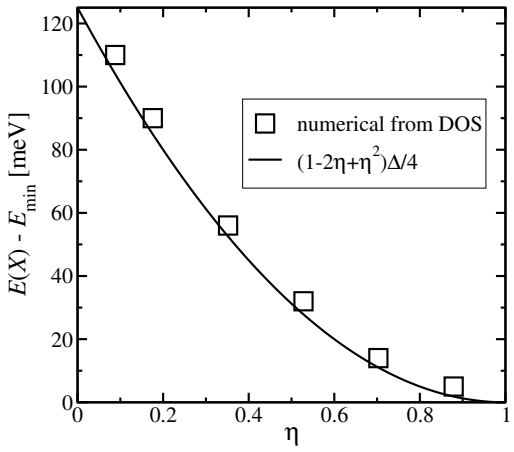

Figure 5: Energy at the X point relative to the value at the minimum. Solid line is a theoretical prediction based on (8).

(dotted lines), with strain dependent transversal effective masses (11), (12) and strain dependent longitudinal mass $m_l(\eta)$. The dependence of $m_l(\eta)$ on η is taken in the form [2, 3]:

$$m_l(\eta)/m_l = \begin{cases} (1-\eta^2)^{-1} & , \quad |\eta| < 1 \\ (1 - 1/|\eta|)^{-1} & , \quad |\eta| > 1 \end{cases} \quad (18)$$

Without the non-parabolicity parameter included, considerable deviations in the ratio of the numerical DOS to its analytical value is observed at higher energies. The ratio becomes much closer to unity, if the non-parabolicity correction due to stress dependent $\alpha(\eta)$ is taken into account in the analytical DOS (Fig. 4, solid lines). However, a deviation of the numerical DOS from the analytical model with the stress dependent non-parabolicity parameter is observed for energies larger than k_BT at high stress value. This happens due to the fact that the energy difference between the value at the minimum and the value at the X point decreases with stress (see Fig. 1). A pronounced peak in the numerical DOS appears, which corresponds to the flat dispersion close to X. The energy value of the peak is shown in Fig. 5 for different stress values and compared with theoretical predictions based on (8). For stress values larger than 3 GPa the energy difference from the minimum to the value at the X point becomes smaller than $2 \times k_BT$, as seen from Fig. 5, and a full-band description is required [2]. Through the modification of the density of the after-scattering states, the non-parabolicity parameter affects scattering rates and thus the mobility of the system. As example we consider the mobility in a double-gate FET sketched in Fig. 6. The subband energies and corresponding wave functions are calculated from the Schrödinger equation coupled self-consistently with the Poisson equation, for each value

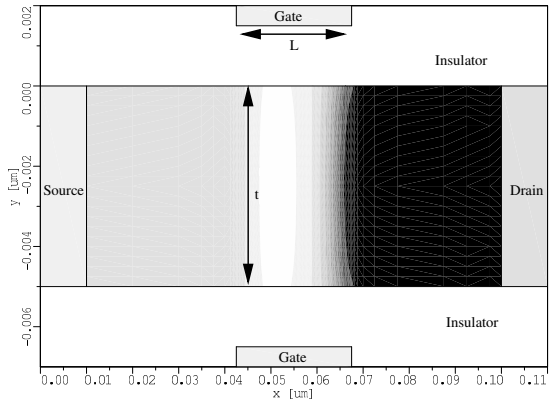

Figure 6: Sketch of a double-gate MOSFET structure. The contour plot shows the potential profile of the conduction band at the source-drain bias of 0.3 V and gate voltage 0.0 V.

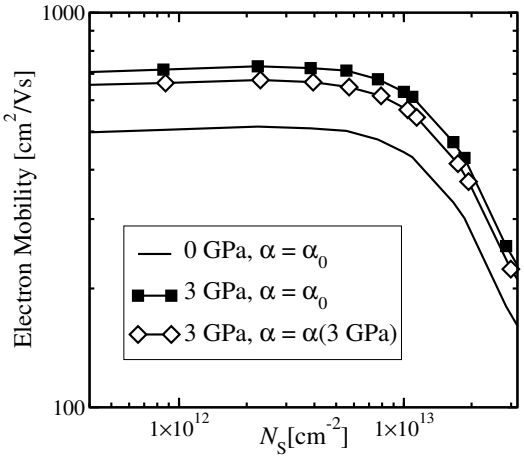

Figure 7: Mobility in a 3 nm thick SOI FET at 3 GPa [110] stress computed with and without stress dependence of the non-parabolicity parameter.

of the effective field. The wave functions are then used to calculate the scattering rates. Our transport calculations account for electron-phonon interactions [5, 7] and surface roughness scattering, which are the dominant mechanisms determining the mobility in the region of high effective fields. We use the original formulation by Prange and Nee [8, 9, 10] of the surface roughness scattering matrix elements.

Results of the mobility simulations in an ultra-thin body FET with strain along the [110] direction, with and without stress-dependence of the the non-parabolicity parameter taken into account, are shown in Fig. 7 together with the mobility in an unstrained SOI FET. Due to the stress dependence of the transversal mass the mobility the in UTB FET under uniaxial stress is significantly enhanced. However, when the stress dependence of the non-parabolicity parameter is included, the mobility enhancement is suppressed by almost 25% in a 3 nm thick SOI FET at a stress level of 3 GPa (Fig. 7).

CONCLUSION

The dependence of the non-parabolicity parameter on shear strain is analyzed for the first time. An analytical expression of the non-parabolicity parameter stress dependence is obtained and verified by comparing the corresponding DOS to the numerical DOS obtained with the empirical pseudo-potential method. The stress dependence of the non-parabolicity parameter results in almost 25% decrease of the mobility enhancement in a 3 nm thin SOI FET at high stress levels.

ACKNOWLEDGMENT

This work, as part of the European Science Foundation EUROCORES Programme FoNE, was supported by funds from FWF (project I79-N16), CNR, EPSRC and the EC Sixth Framework Programme, under Contract N. ERAS-CT-2003-980409, and by the Austrian Science Fund, project P19997-N14.

REFERENCES

[1] K. Uchida, T. Krishnamohan, K. C. Saraswat, and Y. Nishi, in *IEDM Techn. Dig.* (2005), pp. 129–132.

[2] E. Ungersboeck *et al.*, IEEE Trans.Electron Devices **54**, 2183 (2007).

[3] V. Sverdlov, E. Ungersboeck, H. Kosina, and S. Selberherr, in *Proc. EUROSOI 2007* (January, 2007), pp. 39–40.

[4] J. C. Hensel, H. Hasegawa, and M. Nakayama, Physical Review **138**, A225 (1965).

[5] C. Jacoboni and L. Reggiani, Reviews of Modern Physics **55**, 645 (1983).

[6] I. Balslev, Physical Review **143**, 636 (1966).

[7] P. J. Price, Ann.Phys. **133**, 217 (1981).

[8] R. E. Prange and T. W. Nee, Physical Review **168**, 779 (1968).

[9] M. V. Fischetti *et al.*, J.Appl.Phys. **94**, 1079 (2003).

[10] D. Esseni, IEEE Trans.Electron Devices **51**, 394 (2004).